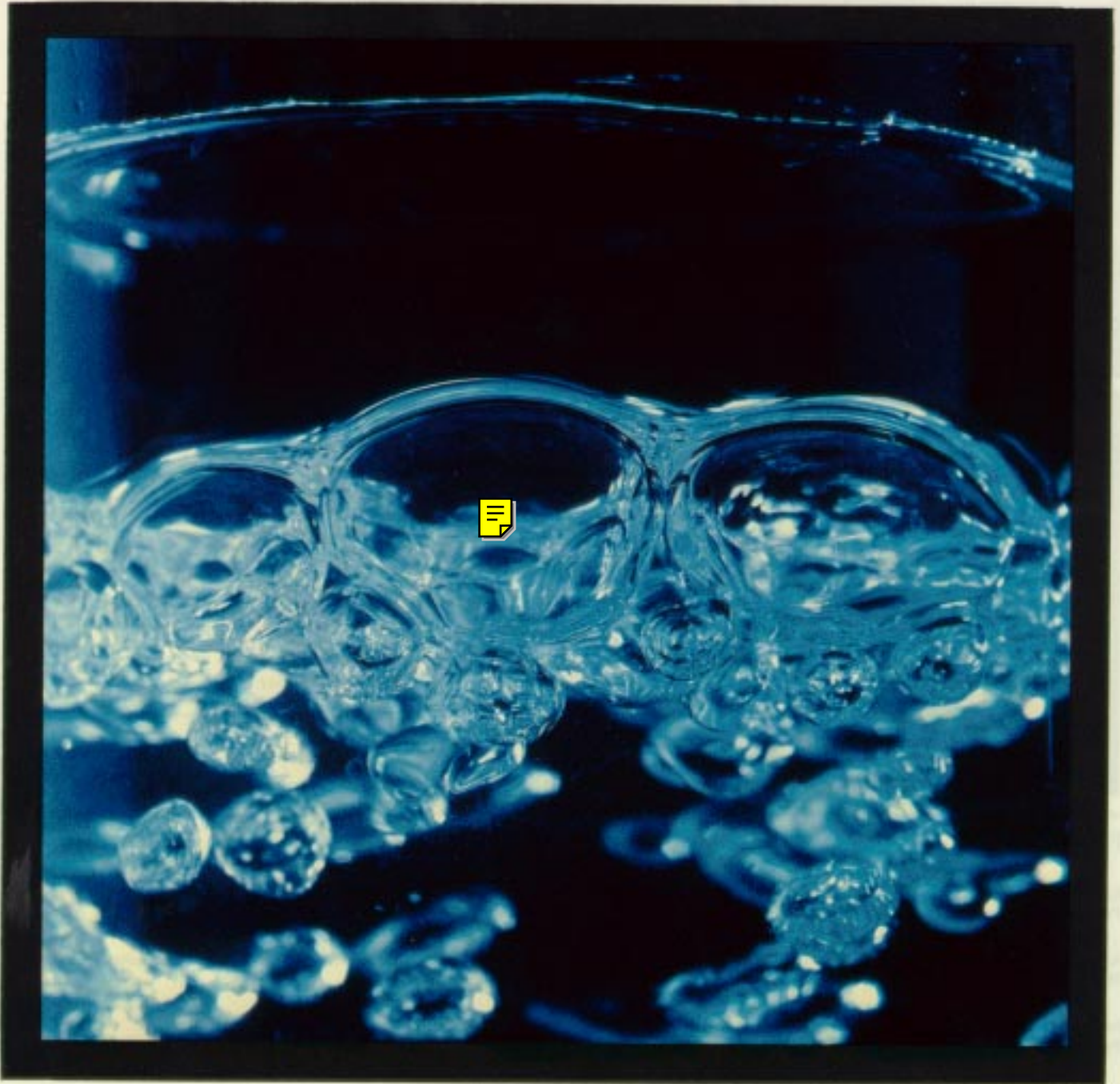


two phase flow

Complex steam-water flows occur in a pot of boiling water just as they do in a pressurized-water reactor during a loss-of-coolant accident. Successful methods for analyzing these two-phase flows were first developed at Los Alamos National Laboratory.

by Dennis R. Liles

BRINKTUA



Many natural and manmade situations provide examples of two-phase flow—bubbles rising in a carbonated drink, raindrops falling through the air, gasoline and air reacting in an automobile engine, water and steam circulating through a nuclear reactor. Common to all two-phase flows is the existence of discernible interfaces, or boundaries, that separate one phase from the other. Whether the flow involves two immiscible liquids, a liquid and a solid, a liquid and a vapor, or a solid and a vapor, the interracial topology constantly changes as the phases interact, exchanging energy, momentum, and often mass. These interactions and changes in interracial topology are the most difficult aspect of two-phase flow to model. Although little progress has been made in describing the detailed dynamics from first principles, macroscopic properties of two-phase flows can be determined satisfactorily from approximate models. Such models are essential for the safe and economic operation of a host of commercial systems—power generation, heating and cooling, material processing, and transport systems, to name a few.

Here we focus attention on the steam-water flows that may occur during transients in pressurized-water reactors, but the methods presented are applicable to liquid-solid and liquid-liquid flows as well. The Laboratory has been a leader in the development of sophisticated numerical techniques for analysis of multiphase flows and in the construction of computer codes based on these techniques. Applications of these codes are described in the four articles that follow. In this article, we discuss the basic principles incorporated in models for liquid-vapor flows and illustrate the numerical techniques for solving the resulting equations. The level of sophistication described here is typical of that in **TRAC**, the large systems code developed, at the request of the Nuclear Regulatory Commission, by Los Alamos for light-water reactor safety analysis.

Flow Regimes

Two-phase flows exhibit various flow regimes, or flow patterns, depending on the relative concentration of the two phases and the flow rate. A simple but generally adequate set of descriptive phrases for most of the important liquid-vapor flow regimes consists of bubble flow, slug flow, churn flow, annular flow, and droplet flow.

Bubble flow describes the flow of distinct, roughly spherical vapor regions surrounded by continuous liquid. The bubble diameter is generally considerably smaller than that of the

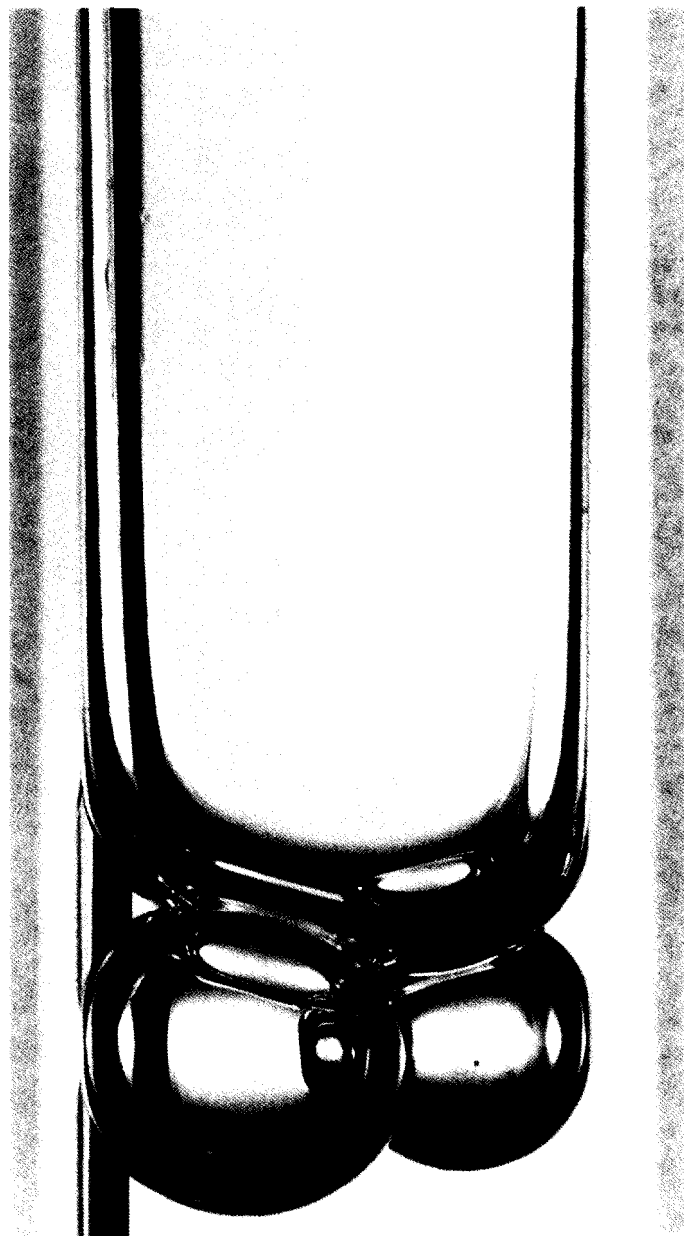


Fig. 1. Photograph of slug flow.

container through which they flow. Bubble flow usually occurs at low vapor concentrations.

If the vapor and liquid are flowing through a pipe, bubbles may coalesce into long vapor regions that have almost the same diameter as the pipe (Fig. 1). This is called slug flow.

At moderate to high flow velocities and roughly equal

concentrations of vapor and liquid, the flow pattern is often very irregular and chaotic. If the flow contains no distinct entities with spherical or, in a pipe, cylindrical symmetry, it is said to be churn flow.

At high vapor concentration, the liquid may exist as a thin film wetting the pipe wall (annular flow) or as small, roughly spherical droplets in the vapor stream (droplet flow). If both a thin film and droplets exist, the flow is described as annular-droplet flow.

All these regimes can be exhibited by liquid flowing vertically upward through a heated tube (Fig. 2). Each regime requires somewhat different modeling because the dominant interactions between liquid and vapor change their character from one regime to another.

Everyone has observed some of these flow patterns in the home. For example, as a pot of water is heated, small bubbles form on the hot bottom surface. These grow, detach, and rise to the surface, driven by their buoyancy and by liquid convection. When the bubbles reach the surface, they break and send tiny droplets upward in a visible mist. Interaction of the small waves resulting from the bubbles' collapse produces larger droplets. Initially, these accelerate upward from the surface but are too large to be carried very far by the rising steam, so they fall and splash back onto the liquid. Even this mundane situation is chaotic and complicated, and its simulation presents interesting problems.

Anyone who has attempted to drink liquid from an inverted pop bottle has experienced slug flow. The liquid exits as a series of chunks rather than a smooth stream, and the air that replaces the liquid enters the bottle as a series of vapor slugs. The same general formulation that describes bubbles rising in a pot can be used to describe the flow of liquid from the inverted bottle or the complex steam-water flows in a pressurized-water reactor.

Steam-Water Flows in Pressurized-Water Reactors

During normal operation of a pressurized-water reactor, water in the primary cooling system is at a pressure of about 150 bars (about 150 atmospheres) and a temperature of about 590 kelvin (about 600°F). The water, circulated by large centrifugal pumps, flows into the reactor vessel, down an annulus, up through the core where it is heated by the fuel rods, into an upper plenum, and out of the vessel. The hot

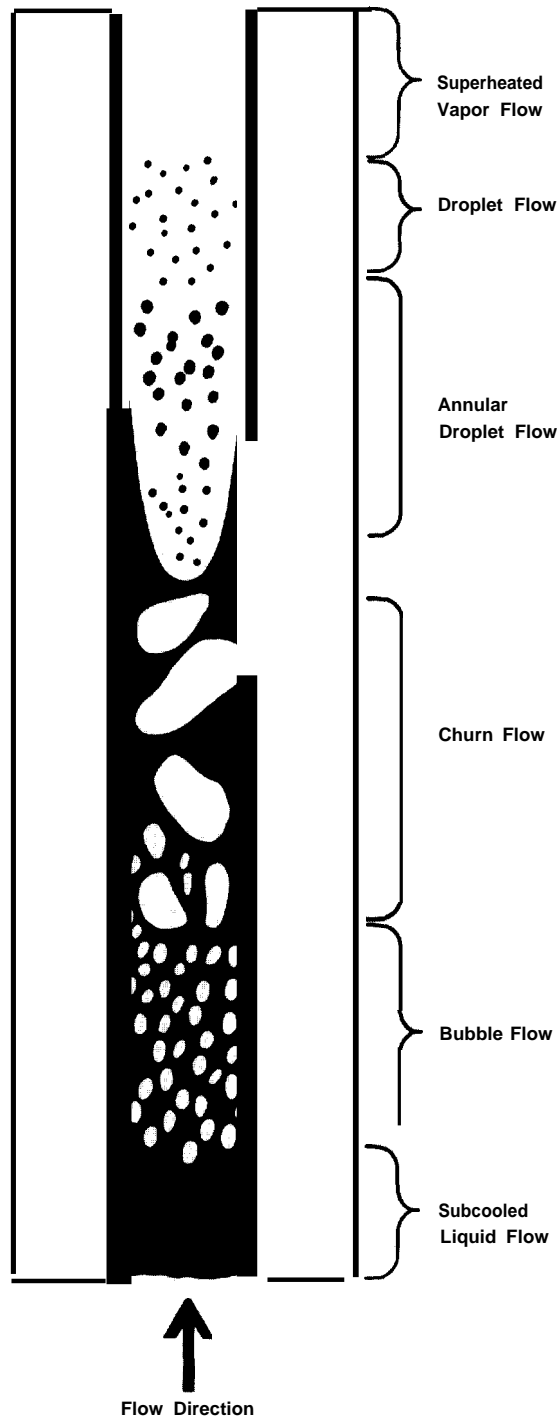


Fig. 2. Flow regimes exhibited by water flowing vertically upward through a heated tube at moderate to high flow velocities.

water, still liquid, flows from the reactor vessel through a heat exchanger, called the steam generator, where the energy is removed from the primary system. The cooler liquid returns to the pump and the process continues. The water on the secondary side of the steam generator is at a lower pressure and quickly boils. The steam powers a turbine that drives a generator, and is then recovered from the turbine, condensed in another heat exchanger, and returned to the secondary system pumps.

Now suppose that a pipe breaks in the primary system. The pressure drops and the superheated water flashes to steam. As the pressure drops further, emergency core-cooling systems are activated to prevent overheating of the core. These systems inject cold water into the pipes connected to the reactor vessel. Both vaporization and condensation may occur simultaneously in different regions of the primary system and produce complex, turbulent steam-water flows. To follow the evolution of these flows and predict their effectiveness in cooling the core requires detailed models of the two-phase flow.

The Two-Fluid Model

Analysis of two-phase flow begins with the most general principles governing the behavior of all matter, namely, conservation of mass, momentum, and energy. These principles can be expressed mathematically at every point in space and time by local, instantaneous field equations. However, exact solution of these equations is almost impossible and very expensive, requiring the tracking of many convoluted liquid-vapor interfaces that change continuously in time. Instead, the usual procedure is to average the local, instantaneous equations in either time or space, or both. Although we lose information in the process, the resulting equations yield accurate solutions to a wide variety of practical problems so long as the averaged variables bear some resemblance to the actual situation, that is, so long as the flow is not too chaotic.

During the averaging, the two phases may be treated together to obtain averaged variables for a two-phase mixture; alternatively, treating each phase separately, we obtain averaged variables for both phases. The latter procedure yields the two-fluid model, which is a bit more general and useful. (The mixture model can be derived from the two-fluid model.)

A usual two-fluid model consists of six field equations: averaged mass, momentum, and energy equations for the

liquid and another set of three for the vapor. For example, integrating across the cross section of our heated tube (Fig. 2) at some particular time, through regions with liquid and regions with vapor, we obtain area-averaged conservation equations for the liquid and the vapor. Or, integration over a small volume element provides volume-averaged equations. We could also integrate over a period of time at some particular location in the tube to obtain time-averaged conservation equations. Finally, additional variables are introduced into the averaged conservation equations, namely, the volume (or area) fraction of the vapor a_1 and of the liquid a_2 for a given region. Because the flowing material is either vapor or liquid, a_1 and a_2 are not independent. Rather $a_1 + a_2 = 1$.

Other procedures (for example, Boltzmann statistical averaging) may be followed to obtain usable field equations, but these are the most common. Fortunately, all the averaging techniques produce effectively identical sets of equations, at least one-dimensional equations.

The field equations are usually derived by assuming that the interface separating the phases has zero thickness and zero mass, and hence cannot store momentum or kinetic and thermal energy. To complete the field equations, mass, momentum, and energy fluxes of one phase must be connected across the interface to the corresponding fluxes of the other phase. With suitable simplifications, these connections are usually effected with “jump conditions.”

We will illustrate application of the two-fluid model to vapor-liquid flow with the field equations for conservation of mass and the appropriate jump condition. For flow of a single phase in the absence of sources and sinks, conservation of mass is expressed as

$$\frac{\partial \rho}{\partial t} + \nabla \cdot \rho \vec{v} = 0 ,$$

where ρ is the density of the fluid and \vec{v} is its velocity. For the case at hand, we need two mass-conservation equations, one for each phase, and must include the possibility of vaporization and condensation at the rates Γ_1 and Γ_2 , respectively. We obtain the following mass-balance equations for vapor and liquid. (Averaging symbols have been omitted for simplicity.)

$$\frac{\partial (\alpha_1 \rho_1)}{\partial t} + \nabla \cdot (\alpha_1 \rho_1 \vec{v}_1) = \Gamma_1 \quad (1)$$

and

$$\frac{\partial (\alpha_2 \rho_2)}{\partial t} + \nabla \cdot (\alpha_2 \rho_2 \vec{v}_2) = \Gamma_2 . \quad (2)$$

Conservation of mass implies that the jump condition at the interface is

$$\Gamma_1 + \Gamma_2 = 0 .$$

That is, production of vapor at the interface depletes the liquid phase by an equal amount.

The field equations based on conservation of energy and momentum, although similar, are more complicated and are often formulated with additional simplifying assumptions. For example, we often ignore turbulent stresses in the momentum equation and turbulent work terms in the energy equation,

Constitutive Relations

The field equations are an expression only of conservation principles; they describe neither the thermodynamic properties of the materials involved nor the interactions between the phases and between each phase and the medium in which the flow occurs. Completion of the analysis requires “constitutive relations” that describe these properties and interactions.

For the steam-water flows that are of interest here, the constitutive relations that are the most difficult to specify properly are those describing the interactions between the phases. Consider, for example, the averaged equation for conservation of mass of the vapor phase (Eq. 1). Expressed in words, this equation simply states that, within a volume element, the temporal change in the vapor mass equals the rate of vapor production minus the exiting vapor flux.

However, this equation cannot be applied to a real problem until we have a constitutive relation that specifies the rate of vapor production.

A number of basic models have been used to determine this variable. Early vapor-liquid studies were often based on a thermodynamic equilibrium model. This model includes the assumption that when two phases coexist, both must be at the saturation temperature. Thermodynamic equilibrium is maintained in this model by balancing pressure changes with sufficient vaporization or condensation,

Although adequate to describe many situations, this model

fails when the effects of thermodynamic disequilibrium are important. Such is the case, for example, in a reactor core during accident conditions. Droplets of water at temperatures close to saturation may be entrained by steam at a temperature much higher than saturation. To evaluate properly the cooling effects of the steam-droplet mixture on the fuel rods, the temperature of the droplets and of the steam must be considered separately.

INTERFACIAL MASS AND ENERGY EXCHANGE. In our studies of transient reactor behavior, we use a simple non-equilibrium phase-change model based on a thermal-energy jump condition at the vapor-liquid interface. At a region in space where both phases exist, we specify an energy balance between the phases at the interface (Fig. 3). Because we assume that the interface cannot store thermal energy, the net energy transferred to the interface by vapor and liquid must be used up by vaporization (or condensation). Thus the rate of vapor production Γ_1 is given by

$$\frac{q_1 + q_2}{\Delta H} = \Gamma_1 . \quad (3)$$

where q_1 and q_2 are the rates of heat transfer to the interface

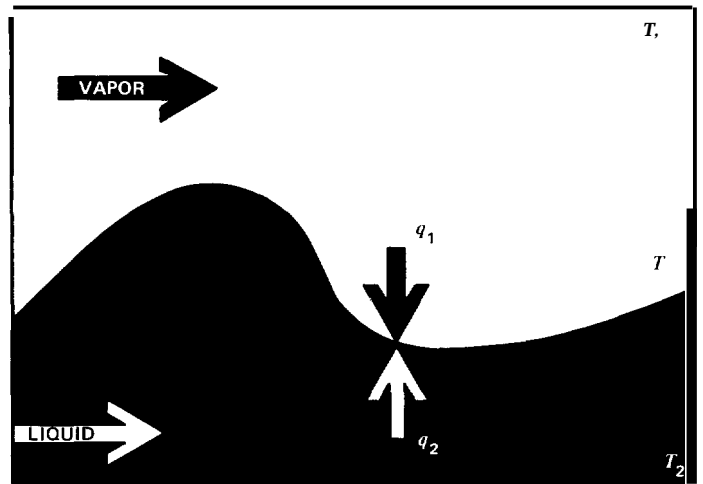


Fig. 3. Mass and thermal energy are exchanged between vapor and liquid through a massless interface. Because the interface cannot store thermal energy, the net energy transferred to the interface, $q_1 + q_2$, must result in vaporization or condensation.

from the vapor and the liquid, respectively, and ΔH is the enthalpy difference between the phases. If the interface is assumed to be at the local saturation temperature T_{sat} , then $\Delta H = L$, the heat of vaporization of the material at the local pressure.

Expressions for the interracial heat transfers are obtained by assuming that each phase has an average temperature, denoted by T_1 and T_2 , and by applying Newton's law of cooling.

$$q_1 = h_1 A (T_1 - T_{sat})$$

and

$$q_2 = h_2 A (T_2 - T_{sat}) .$$

The proportionality constants h_1 and h_2 are the heat-transfer coefficients between the interface and vapor and between the interface and liquid, respectively, and A is the interracial area. Substituting these expressions into Eq. 3, we obtain Γ_1 as a function of h_1 , h_2 , and A .

$$\Gamma_1 = \frac{A}{L} [h_1 (T_1 - T_{sat}) + h_2 (T_2 - T_{sat})] . \quad (4)$$

The temperatures T_1 and T_2 can be calculated from the coupled field equations and may be regarded as known. However, the interracial heat-transfer coefficients and the interracial area depend on the interracial topology, which is not specified in our averaged two-fluid model.

We usually obtain values for h_1 , h_2 , and A by first determining the local flow regime from a steady-state flow-regime map. Such a map relates observed flow regimes to local flow conditions, that is, to volume fraction of one or the other phase and to flow velocities of both phases. (These variables are available from the field equations.) Figure 4 shows a particularly simple flow-regime map based on observations of upward air-water flow in a vertical pipe. Having determined the local flow regime, we use empirical correlations appropriate to that regime to obtain values for h_1 , h_2 , and A . Although this technique cannot be fully justified from first principles, it is relatively simple and often supplies reasonable answers to complex problems.

Sometimes further information may be needed to use the customary empirical correlations for h_1 , h_2 , and A . For example, the flow-regime map may specify droplet flow, but a

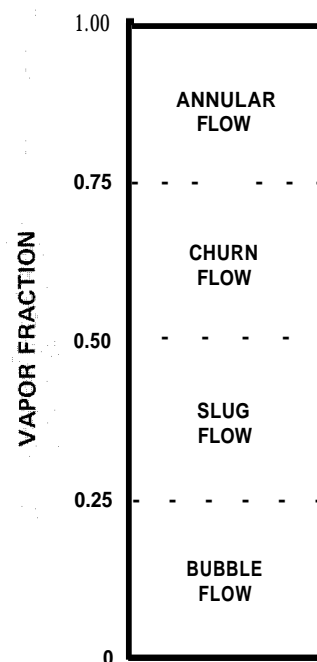


Fig. 4. Observed flow-regime map for upward air-water flow in a vertical pipe. The flow regime is independent of flow velocity and depends only on the vapor fraction. As the vapor fraction increases (and the number and size of the bubbles increase), collisions between the bubbles become more frequent, and they coalesce into slugs. At higher vapor fraction, vapor slugs cannot exist, and churn flow sets in. Finally, an annular-droplet flow occurs at very high vapor fraction.

mean droplet size is required. A local approximation based on a Weber number criterion is often used to specify an average droplet diameter d . This criterion is an expression of the idea that, for droplet flow to exist, disruptive forces (forces due to relative motion of droplets and vapor that tend to break up the droplets) and restoring forces (due to surface tension σ) must be in a certain ratio. Expressed mathematically,

$$\frac{\rho_1 (v_1 - v_2)^2 d_{max}}{\sigma} = We ,$$

where d_{max} is the maximum droplet size and We , the Weber number, is some constant. We use $d \approx 0.5 d_{max}$.

The Weber number criterion does not take into account the existence of a spectrum of droplet sizes, velocities, and cooling rates; in addition, it sometimes predicts nonphysical results. For example, consider subsonic droplet flow in a convergent-divergent nozzle. Applied to large drops as they enter the convergent section, the Weber number criterion gives a reasonably accurate estimate of their largest size as they break up.

However, further downstream in the region of slower flow the same criterion predicts coalescence that does not in fact occur (Fig. 5).

Simplifications similar to those delineated above are included in most current computer codes. Fortunately, for many problems of interest, accuracy of the interracial terms need only be sufficient to provide reasonable overall results. However, work is progressing on replacing some of these approximations with additional differential equations for a characteristic length (or area) field to be convected around with the flow. These equations will provide a better history of droplet evolution and more realistic estimates of the interracial interactions.

INTERFACIAL MOMENTUM EXCHANGE. We have discussed in some detail the development of constitutive relations that describe the interracial exchange of mass (by the mechanism of phase change) and its relationship to the interracial exchange of energy. Another important interracial interaction that must be taken into account is exchange of momentum between the two phases. This exchange arises because, in general, the two phases do not travel at the same velocity. (Witness the upward flow of steam bubbles in a pot of heated water or of carbon dioxide bubbles in a newly opened pop bottle.) A full description of the interracial momentum transfer requires consideration of various phenomena, including, among others, “added-mass” effects, Basset forces, steady-state drag forces, and phase-change thrust effects. However, the customary procedure is to consider only the last two, which are the local forces that dominate most problems. Both are dependent on the local flow regime, and again, flow-regime maps and empirical correlations are invoked.

A source of error in most calculations should be pointed out. Averaging operators, which have not here been indicated explicitly, can be important in formulating models because the averaged equations include many quantities that are averages of products. But in most calculations, it is assumed, for example, that $\langle \rho v^2 \rangle = \langle \rho \rangle \langle v \rangle \langle v \rangle$, where $\langle \quad \rangle$ and $\langle \quad \rangle$ denote a spatial

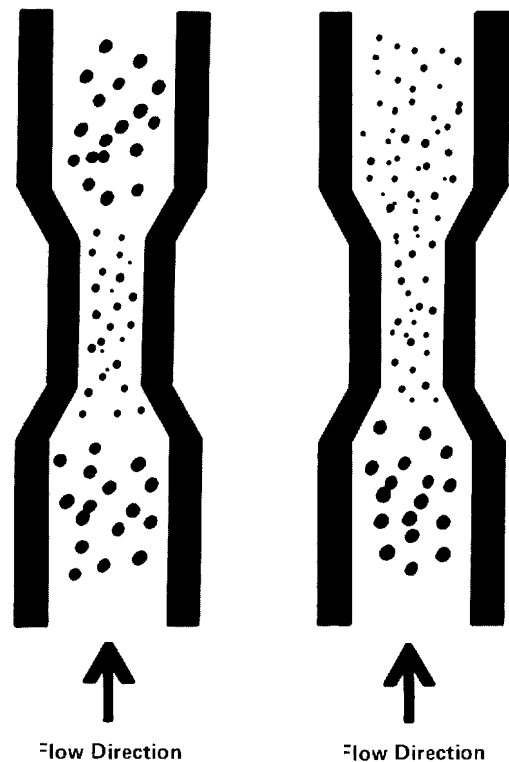


Fig. 5. A comparison of predicted and actual subsonic droplet flow through a convergent-divergent nozzle. (a) The Weber number criterion predicts that large drops break up into small drops in the convergent section and coalesce into large drops in the divergent section. (b) In reality, the small drops do not coalesce in the divergent section.

average. This assumption is strictly valid only if the density and velocity are constant across the region where the averaging is effected. (Such errors can be corrected for if information about the density and velocity profiles is available.) We raise the point here because the error so introduced is larger for momentum fluxes (ρv^2 terms) than for mass fluxes (ρv terms).

INTERACTIONS WITH CONTAINING MEDIUM. The interactions between each phase and the medium through which they flow (such as pipe walls and structures within a reactor vessel) are another set of necessary constitutive relations. Wall shear and wall heat transfer must be modeled with some accuracy to obtain realistic analyses of transient reactor response. Particular attention must be paid to modeling the extreme variation (by orders of magnitude) of heat transfer from the fuel rods as local flow conditions change. Correlating procedures using Newton’s law of cooling are customary, but the resulting functions that specify the heat-transfer coefficients to the liquid and vapor are complicated and not always well supported by experimental data.

Numerical Solution Techniques

Even the simplified models for two-phase flow described above are fairly complicated. The two-fluid model includes six

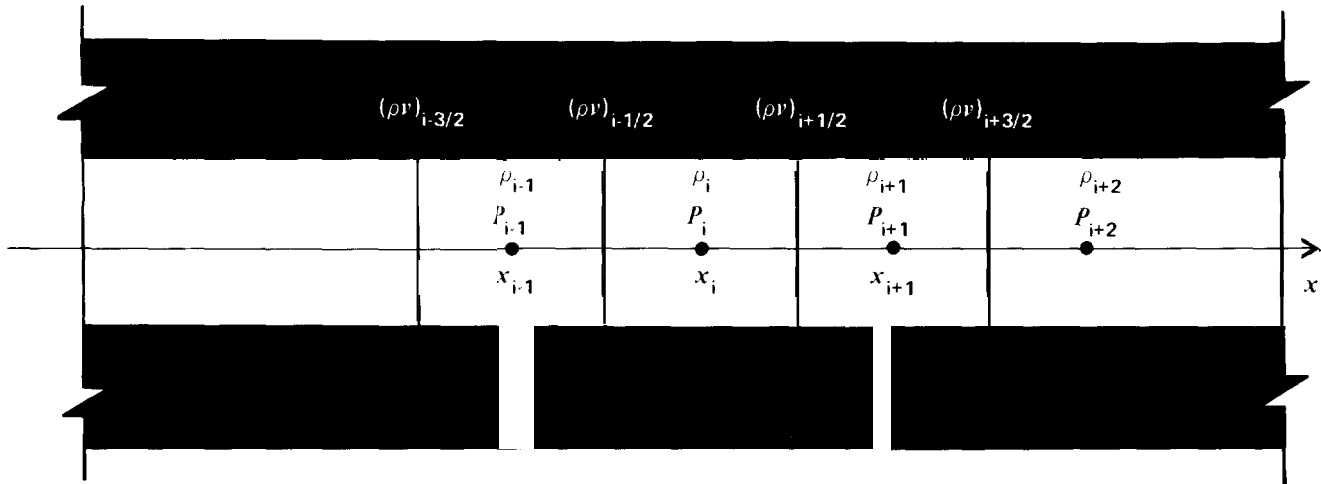


Fig. 6. To apply the method of finite differences to one-dimensional flow, the x -axis is divided into equal intervals with

coupled partial differential equations and numerous thermodynamic and constitutive equations. Solutions for specific problems are obtained by using numerical techniques and high-speed computers. The Laboratory's greatest contribution to analysis of two-phase flow is the development of numerical solution techniques and large-scale computer codes. Francis H. Harlow and his associates were among the first to compute these flows successfully with a two-fluid model.

The partial differential equations that represent the conservation laws cannot be solved directly with a (digital) computer. Instead, these equations must be approximated by algebraic equations. We will use the method of finite differences to solve a set of equations describing the flow of a single phase through a pipe. We assume that the flow can be described in sufficient detail in one dimension, along the pipe axis. The set consists of equations for conservation of mass and momentum and a thermodynamic equation of state.

$$\frac{\partial \rho}{\partial t} + \frac{\partial(\rho v)}{\partial x} = 0 \quad (5)$$

$$\frac{\partial(\rho v)}{\partial t} + \frac{\partial(\rho v^2)}{\partial x} = -\frac{\partial P}{\partial x} \quad (6)$$

and

$$\rho = \rho(P) \quad ,$$

where ρ is the microscopic density, v is the velocity, and $\rho(P)$ is some (known) function of the pressure P .

For convenience, we divide the distance along the x -axis into equal finite intervals, or cells, of length Δx and denote the midpoints by x_i . The thermodynamic variables ρ and P are defined at the cell midpoints and the mass flux ρv at the cell edges (Fig. 6). We also divide the time coordinate into equal intervals of duration Δt with endpoints denoted by t_j . Super-

scripts and subscripts on the dependent variables indicate, respectively, time and location.

The temporal term of our mass-conservation equation (Eq. 5) may be approximated by

$$\frac{\partial \rho}{\partial t} = \frac{\rho_i^{j+1} - \rho_i^j}{\Delta t}$$

and the spatial term by

$$\frac{\partial(\rho v)}{\partial x} = \frac{(\rho v)_{i+1/2} - (\rho v)_{i-1/2}}{\Delta x} \quad .$$

(Note that we have not yet specified the times for the spatial term. We shall address this issue below.) Our approximation for Eq. 5 in the cell bounded by $x_{i-1/2}$ and $x_{i+1/2}$ is thus given by

$$\frac{\rho_i^{j+1} - \rho_i^j}{\Delta t} = -\frac{(\rho v)_{i+1/2} - (\rho v)_{i-1/2}}{\Delta x} \quad (8)$$

We could approximate our momentum-conservation equation (Eq. 6) over the same cell, obtaining

$$\frac{(\rho v)_{i+1/2}^{j+1} - (\rho v)_{i+1/2}^j}{\Delta t} + \frac{(\rho v^2)_{i+1/2} - (\rho v^2)_{i-1/2}}{\Delta x} = -\frac{P_{i+1/2} - P_{i-1/2}}{\Delta x} \quad (9)$$

We choose instead to approximate it over the cell bounded by x_i and x_{i+1} , and obtain

$$\frac{(\rho v)_{i+1/2}^{j+1} - (\rho v)_{i+1/2}^j}{\Delta t} + \frac{(\rho v^2)_{i+1} - (\rho v^2)_i}{\Delta x} = -\frac{P_{i+1} - P_i}{\Delta x} \quad (10)$$

(Again, we have not yet specified the times for the spatial terms.)

There are two reasons for choosing to "stagger" the mass and momentum cells. First, Eq. 9 specifies pressures at the cell edges rather than at the cell centers where we have defined

them. Solving this problem involves use of pressures spanning three cells (P_{i+1} and P_{i-1}). In contrast, the pressures specified in Eq. 10 span only two cells, a situation that greatly improves the solvability of the system of linear equations (improves the diagonal dominance of the resulting matrices). Second, notice that mass flux is the dependent variable common to Eq. 8 and Eqs. 9 or 10. Both Eq. 8 and Eq. 10 specify this variable at cell edges, whereas Eq. 9 specifies it at cell centers. Therefore, mass flux values from Eq. 10 can be substituted directly into Eq. 8, a convenient situation.

The numerical analyst must select a numerical technique and a difference scheme, such as that represented by Eqs. 8 and 10, that exhibit accuracy and stability. The term accuracy means that, as Δt and Δx are made smaller and smaller, the numerical results are better and better approximations of the exact solution to the original differential equations. Stability means that the results show no unbounded growth of errors. Generally, stability depends on the choice of Δt and Δx .

We can decide how to time-difference the spatial terms in Eqs. 8 and 10 on the basis of stability criteria. Let us assume for the moment that we are using what is known as a fully explicit difference scheme, that is, all the spatial terms are specified at time t_j . It can be shown that our technique is then stable only if everywhere

$$\frac{(v + C)\Delta t}{\Delta x} < 1, \quad (11)$$

where C is the local sound speed $(\partial P/\partial \rho)^{1/2}$ at constant entropy. We can develop a feel for why this is so by examining the consequences of violating the criterion. Then, for small velocities ($v \ll C$), $\Delta t > \Delta x/C$. For example, we will set Δt equal to $2\Delta x/C$. During a time interval of this duration, a small, narrow pressure pulse at x_i will travel a distance $2\Delta x$ (the wave speed of the pulse is C) to x_{i+2} . At the end of the time interval, at t_{j+1} , the mass flux at $x_{i+3/2}$, and hence certainly at $x_{i+1/2}$, should be affected. But Eq. 10, containing pressure values at t_j , does not reflect the influence of the pulse. In fact, calculated results based on time intervals violating the criterion of Eq. 11 will quickly show exponential growth of errors and become meaningless.

Because the sound speed is high for liquids, the stability criterion of Eq. 11 restricts us to quite short time intervals. We prefer to use instead a semi-implicit technique: in the momentum-conservation equation, to specify the pressures at t_{j+1} and

the momentum fluxes at t_j , and, in the mass-conservation equation, to specify the mass fluxes at t_{j+1} . Through similar arguments based on mass transport, it can be shown that this semi-implicit technique will be stable only if $v\Delta t/\Delta x < 1$, a much less restrictive criterion.

Applying the semi-implicit difference scheme to Eqs. 8 and 10 and rearranging, we arrive at the following system of equations.

$$\rho_i^{j+1} = \rho_i^j - \frac{\Delta t}{\Delta x} \left[(\rho v)_{i+1/2}^{j+1} - (\rho v)_{i-1/2}^{j+1} \right] \quad (12)$$

and

$$(\rho v)_{i+1/2}^{j+1} = (\rho v)_{i+1/2}^j - \frac{\Delta t}{\Delta x} \left[(\rho v^2)_{i+1}^j - (\rho v^2)_i^j + P_{i+1}^{j+1} - P_i^{j+1} \right]. \quad (13)$$

A problem remains: we need values for the momentum fluxes. First, note that momentum fluxes can be calculated from mass fluxes, that is, $\rho v^2 = (\rho v)^2/\rho$. Then, we must decide what mass fluxes to use. Stability considerations demand that we use "upwind" mass fluxes. That is, if v_{i+1} is positive, we calculate $(\rho v^2)_{i+1}$ from the mass flux at $x_{i+1/2}$. If v_{i+1} is negative, the mass flux at $x_{i+3/2}$ is used.

An equation for ρ_i^{j+1} is obtained by substituting expressions for $(\rho v)_{i+1/2}^{j+1}$ and $(\rho v)_{i-1/2}^{j+1}$ (both provided by versions of Eq. 13 at $x_{i+1/2}$ and $x_{i-1/2}$) into Eq. 12. The reader so enthusiastic as to attempt the algebra will generate an equation for ρ_i^{j+1} in terms of known quantities (quantities at t_j) and the pressures $(P)_{i+1}^{j+1}$, P_i^{j+1} , and $(P)_{i-1}^{j+1}$. At this point, we linearize our equation of state.

$$\rho_i^{j+1} = \rho_i^j + \frac{d\rho}{dP} (P_i^{j+1} - P_i^j), \quad (14)$$

where $d\rho/dP$ is obtained from Eq. 7. Combining Eq. 14 with our final equation for ρ_i^{j+1} results in an equation for pressure with a tridiagonal band structure in P_{i-1} , P_i and P_{i+1} . Solution of this equation provides us with pressures at t_{j+1} and, hence, with densities and mass fluxes from the equation of state and Eq. 13, respectively. We have now advanced all variables from t_j to t_{j+1} . The process continues until the time boundary is reached.

Our sample problem is an example of an initial-value and a

boundary-value problem. We must therefore somehow be provided with initial values of p , P , and p_v for all x and with boundary values for all t . For some numerical techniques, inclusion of boundary conditions can be a tricky matter; the requirement that we achieve closure for the linear equations often implies the need for more boundary conditions than are demanded by the original differential equations. Inclusion of boundary conditions in the finite-difference technique illustrated here is generally straightforward. Sufficient boundary conditions for single-phase flow through a pipe consist of the pressures external to the pipe at both ends and the density on the inlet side.

With considerably more tedious detail, the method of finite differences can be applied to the more complicated equations describing two-phase flow. Although it may seem nearly impossible, large computer codes that accurately portray all the complexities of a reactor transient can be constructed with this numerical technique and the models described above. TRAC is an outstanding example of such a code.

The challenges in producing a code like TRAC, which currently contains about 40,000 statements, are numerous; careful assessment of the models and methods is necessary. The results, however, are a tool for describing the complicated two-phase flows in reactors and for providing better estimates of reactor safety. ■



Dennis R. Liles, Leader of the Code Development Group, has worked in the area of reactor safety since joining the Laboratory in 1974 and has been in charge of numerical solution techniques and models for TRAC. After receiving his Bachelor of Science in mechanical engineering from the Georgia Institute of Technology in 1968, he taught in the U. S. Army at Fort Bliss, Texas. He earned a Master of Science in mechanical engineering from the University of Texas at El Paso in 1971 and a Ph.D. in the same field from the Georgia Institute of Technology in 1974. His primary interests are in the physics of two-phase flow and the numerical solution of fluid-dynamics problems. His contributions in both these areas have enhanced the ability of analysts to predict the behavior of nuclear reactors. An active member of the American Nuclear Society, he currently serves on the program committee of its Thermal Hydraulic Group.

FURTHER READING

M. Ishii, *Thermo-Fluid Dynamic Theory of Two-Phase Flow*, *Collection de la Direction des Etudes et Recherches d'Electricite de France*, Vol. 22 (Eyrolles, Paris, 1975).

J. G. Collier, *Convective Boiling and Condensation* (McGraw-Hill Book Co., New York, 1972).

G. W. Govier and K. Aziz, *The Flow of Complex Mixtures in Pipes* (Van Nostrand Reinhold Co., New York, 1972).

D. R. Liles and W. H. Reed, "A Semi-Implicit Method for Two-Phase Fluid Dynamics," *Journal of Computational Physics* 26, 390-407 (1978).

P. J. Roache, *Computational Fluid Dynamics* (Hermosa Publishers, Albuquerque, New Mexico, 1972).

F. H. Harlow and A. A. Amsden, "KACHINA: An Eulerian Computer Program for Multifield Fluid Flows," Los Alamos National Laboratory report LA-5680 (1975).